CONFIDENTIAL

Copy 1
RM L52D08a

RESEARCH MEMORANDUM

SMALL-SCALE TRANSONIC INVESTIGATION OF THE EFFECTS OF PARTIAL-SPAN LEADING-EDGE CAMBER ON THE AERODYNAMIC CHARACTERISTICS OF A 50° 38' SWEPTBACK WING OF ASPECT RATIO 2.98

By William J. Alford, Jr., and Andrew L. Byrnes, Jr.

Langley Aeronautical Laboratory
Langley Field, Va.

NATIONAL ADVISORY COMMITTEE FOR AERONAUTICS

WASHINGTON

June 23, 1952

4

CONFIDENTIAL

NATIONAL ADVISORY COMMITTEE FOR AERONAUTICS

RESEARCH MEMORANDUM

SMALL-SCALE TRANSONIC INVESTIGATION OF THE EFFECTS OF PARTIAL-SPAN LEADING-EDGE CAMBER ON THE AERODYNAMIC CHARACTERISTICS OF A 50° 38' SWEPTBACK WING OF ASPECT RATIO 2.98

By William J. Alford, Jr., and Andrew L. Byrnes, Jr.

SUMMARY

A small-scale transonic investigation of two semispan wings of the same plan form was made in the Langley high-speed 7- by 10-foot tunnel through a Mach number range of 0.70 to 1.10 and a mean-test Reynolds number range of 745,000 to 845,000 to determine the effects of partial-span leading-edge camber on the aerodynamic characteristics of a swept-back wing. This paper presents the results of the investigation of wing-alone and wing-fuselage configurations of the two wings; one was an uncambered wing and the other had the forward 45 percent of the chord cambered over the outboard 55 percent of the span. The semispan wings had 50° 38' sweepback of their quarter-chord lines, aspect ratio of 2.98, taper ratio of 0.45, and modified NACA 64A-series airfoil sections tapered in thickness ratio. Lift, drag, pitching moment, and root-bending moment were obtained for these configurations.

The results indicated that, for the wing-alone configuration, use of the partial-span leading-edge camber provided an increase in maximum lift-drag ratios up to a Mach number of 0.95, after which no gain was realized. For the wing-fuselage combination, the partial-span leading-edge camber appeared to cause no gain in maximum lift-drag ratio throughout the test range of Mach numbers. The lift-curve slopes of the partial-span leading-edge camber configurations indicated no significant change over the basic configurations in the subsonic range but resulted in slight reductions at the higher Mach numbers. No significantly large changes in pitching-moment-curve slopes or lateral center of additional loading were indicated because of the modification. The partial-span leading-edge camber resulted in a slight increase in minimum drag at the higher Mach numbers for the wing-alone configuration

and the increase occurred throughout the Mach number range for the wing-fuselage configuration. The partial-span leading-edge camber modification did not prove as effective in improving the performance characteristics as did twisting and cambering a wing of the same plan form to give a uniform loading at a lift coefficient of 0.25 and a Mach number of 1.10, as was done in a previous investigation.

INTRODUCTION

Previous investigations (refs. 1 and 2) have shown that the performance characteristics (as indicated by $(L/D)_{max}$) of low-aspect-ratio sweptback wings could be substantially improved by twist and camber. From a practical standpoint, however, the use of twist and camber presents several structural problems, particularly when considered for application to a variable-sweep airplane which may require that the inboard wing sections remain symmetrical in order to house the variable-sweep mechanisms. In addition, it is obviously desirable to maintain straight-line elements in the vicinity of the flap and aileron hinge-line locations.

In an attempt to achieve some of the favorable effects of warped wings with a more practical modification applicable to existing swept wings and to variable-sweep airplanes, a wing was arbitrarily modified by drooping the forward 45 percent of the chord of the outboard 55 percent of the semispan to provide essentially the same camber as the warped wing of reference 1 while leaving the trailing 55 percent of the chord of the entire semispan coincident with the chord plane of the flat wing of reference 1. The wing with the drooped leading edge will hereinafter be referred to as the "modified wing," and the uncambered wing shall be called the "basic wing." Because of current interest in all types of wing configurations through the transonic speed range, both wing-alone data and wing-fuselage data were obtained and are presented in this report. The fuselage tested is the same as that of reference 1 and is similar to that of a current research airplane.

This investigation of two semispan wings mounted on a reflection plane was made in the Langley high-speed 7- by 10-foot tunnel through a Mach number range of 0.70 to 1.10 and an angle-of-attack range from -10° to 22°. Lift, drag, pitching moment, and root-bending moment were obtained for these configurations.

COEFFICIENTS AND SYMBOLS

C_L lift coefficient, $\frac{\text{Twice semispan lift}}{qS}$

C_D drag coefficient, $\frac{\text{Twice semispan drag}}{qS}$

C_m pitching-moment coefficient referred to $0.25\bar{c}$, $\frac{\text{Twice semispan pitching-moment}}{qS\bar{c}}$

C_B bending-moment coefficient about axis parallel to relative wind in plane of symmetry, $\frac{\text{Root bending moment}}{q\frac{S}{2}\frac{b}{2}}$

q average dynamic pressure over span of model, $\frac{1}{2}\rho V^2$, lb/sq ft

S twice wing area of semispan model, 0.125 sq ft

$\bar{c}$ mean aerodynamic chord of wing, 0.215 ft, based on relationship $\frac{2}{S}\int_0^{b/2} c^2 dy$ (using theoretical tip)

c local wing chord parallel to plane of symmetry, ft

b twice span of semispan model, 0.61 ft

y spanwise distance from plane of symmetry, ft

ρ air density, slugs/cu ft

V stream velocity over model, ft/sec

M effective Mach number, $\frac{2}{S}\int_0^{b/2} cM_a\, dy$

M_l local Mach number

M_a	average chordwise Mach number
R	Reynolds number, $\rho V\bar{c}/\mu$
μ	absolute viscosity, slugs/ft-sec
α	angle of attack of root chord line (parallel to fuselage reference line), deg
d	chordwise distance from wing leading edge parallel to plane of symmetry, ft
z	camber measured from undistorted portion of chord plane, ft
z'	maximum camber measured perpendicular to a line connecting the leading and trailing edge of streamwise sections, ft (see fig. 3)
L/D	lift-drag ratio
$\alpha_{C_{L=0}}$	angle of attack at zero lift coefficient, deg
y_{cal}	lateral center of additional loading (lateral center of lift due to change in angle of attack), $100\frac{\partial C_B}{\partial C_L}$, percent semispan
C_{m_0}	pitching-moment coefficient at zero lift coefficient
$C_{D_{min}}$	minimum-drag coefficient
$C_{L_{C_{D_{min}}}}$	lift coefficient at minimum drag coefficient
$\left[\frac{(L/D)_{max_{mod}}}{(L/D)_{max_{basic}}}\right]$	performance ratio - maximum lift-drag ratio of the modified configuration referred to the maximum lift-drag ratio of the basic configuration
$C_{L_{(L/D)_{max}}}$	lift coefficient at maximum lift-drag ratio

MODELS AND APPARATUS

The basic wing and the modified wing (with partial-span leading-edge camber) were constructed of steel and had 50° 38' of sweepback of their quarter-chord lines, aspect ratios of 2.98, and taper ratios of 0.45. The airfoil sections of the basic wing perpendicular to the 29.3-percent-chord line, where this chord line intersects the streamwise root and tip chords, were NACA $64_{(10)}$A010.9 at the root and NACA $64_{(08)}$A008.1 at the tip. The same 64A airfoil thickness distributions were placed around the mean camber surface of the modified wing. The maximum streamwise thicknesses were 7.4 percent at the root and 5.6 percent at the tip. A two-view drawing of the modified wing-alone configuration is presented in figure 1, and a photograph of a typical configuration mounted on the reflection plane is presented in figure 2. Ordinates of the fuselage used are given in table I.

The modified wing was designed to have the same camber, drooped below the chord plane, in the leading 45 percent chord and over the outboard 55-percent span as the warped wing of reference 1, while leaving the trailing 55 percent of the chord of the entire semispan coincident with the chord plane of the flat wing of reference 1. The chordwise camber variation for several semispan stations, along with spanwise maximum camber variation, is presented in figure 3.

Force and moment measurements were obtained with a strain-gage-balance system and with recording potentiometers. The angle-of-attack values were obtained by means of slide-wire and recording potentiometers.

TESTS

The investigation was made in the Langley high-speed 7- by 10-foot tunnel with the model mounted on a reflection plane (fig. 1) located about 3 inches from the tunnel wall to bypass the wall boundary layer. The reflection-plane boundary-layer thickness was such that, with no model installed, a value of 95 percent of the free-stream velocity was reached at a distance of approximately 0.16 inch from the surface of the reflection plane at the balance center line for all test Mach numbers. This boundary-layer thickness represented a distance of about 4.5-percent semispan for the models tested.

At Mach numbers below 0.93 there was practically no velocity gradient in the vicinity of the reflection plane. At higher Mach numbers, however, the presence of the reflection plane created a high local-velocity field which permitted testing the small models up to a Mach number of 1.10

before choking occurred in the tunnel. The variations of local Mach numbers in the region occupied by the models, obtained from surveys made with no model in position, are shown in figure 4. Effective test Mach numbers were obtained from additional contour charts similar to those shown in figure 4 by the relationship

$$M = \frac{2}{S}\int_0^{b/2} cM_a \, dy$$

From these contours it was determined that Mach number variations (outside of the boundary layer) of less than 0.01 generally were obtained over the region to be occupied by the models below a Mach number of 0.95. These variations had values of 0.05 and 0.07 at Mach numbers of 0.98 and 1.10, respectively. It should be noted that the Mach number variations of this investigation are principally chordwise, whereas the Mach number variations of reference 1 are principally spanwise.

A gap of about 1/16 inch was maintained between the wing-root-chord section and the reflection-plane turntable, and a sponge-wiper seal was fastened to the wing butt on the inner side of the turntable to minimize leakage (ref. 3). Force and moment measurements were made for the wing-alone and wing-fuselage configurations through a Mach number range from 0.70 to 1.10 and an angle-of-attack range from -10° to 22°. The mean-test Reynolds number varied from 745,000 to 845,000 for the range of Mach numbers of these tests as shown in figure 5.

No attempt has been made to apply corrections for jet-boundary or blockage effects. Because of the small size of the models these corrections are believed to be negligible. Corrections due to aeroelastic effects were less than 1.0 percent and were not applied to the data.

In general, the accuracy of the force and moment measurements can be judged by any random scatter of the test points used in presenting the basic data. In applying a technique that utilizes small reflection-plane models mounted in a localized high-velocity field, the reliability of the absolute values of some of the results, particularly the drag values, may be open to question. Experience has indicated, however, that valid determinations of incremental effects, such as those due to lift coefficient, Mach number, or changes in model configuration, normally can be obtained. A more complete evaluation of results obtained by techniques such as that used for the present investigation is given in reference 3.

RESULTS AND DISCUSSION

The basic data for the wing-alone and wing-fuselage configurations are presented in figures 6 and 7. The lift-drag ratios are presented in figures 8 and 9, and a summary of aerodynamic characteristics is given in figures 10 and 11. Unless otherwise stated the discussion is based on the summary curves of figures 10 and 11. The slopes presented have been averaged over a lift-coefficient range of ±0.2.

Lift Characteristics

The lift-curve slopes (figs. 10 and 11) of the modified configuration indicated no significant change over the basic configurations in the subsonic range, but the modification resulted in slight reductions in lift-curve slopes at the higher Mach numbers. The modification also caused small changes in the angle of attack for zero lift and in the lateral center of additional loading (y_{cal}), but these changes are not consistent for the wing-alone and wing-fuselage configurations.

Drag Characteristics

For both the wing-alone and wing-fuselage configurations the wing modification generally resulted in some increase in minimum drag; a maximum increase of 0.006 was obtained with the wing-fuselage combination at a Mach number of 1.10. It should be noted that the values of $C_{D_{min}}$ for the wing-fuselage combinations may be high because of the skin friction and interference drag caused by the additional fuselage surface exposed by the gap between the fuselage and reflection-plane surface. The values of $C_{D_{min}}$ presented in this paper for the basic configurations were noticeably higher than for the comparable configurations of reference 1. These differences could possibly be due to the differences in test facilities, Mach number gradients, and effects of the transonic bump curvature on the effective sweep angle of the model used in reference 1.

The lift coefficient for minimum drag $C_{L_{C_{D_{min}}}}$ generally was slightly more positive for the modified wing than for the basic wing; however, the maximum value of $C_{L_{C_{D_{min}}}}$ obtained with any of the configurations was only about 0.08.

Lift-Drag Ratios

For the wing-alone configurations (fig. 8), the lift-drag ratios for the modified wing were somewhat higher than for the basic wing at lift coefficients above 0.1 and up to a Mach number of 0.95. Above 0.95 a negligible increase was realized. No appreciable change in lift-drag ratios was occasioned by the modification for the wing-fuselage configurations (fig. 9).

The $(L/D)_{max}$ values of the configurations with the modified wing have been referred to the $(L/D)_{max}$ values of the basic configurations, since the significance of a comparison of the absolute values of $(L/D)_{max}$ obtained herein with those obtained for the twisted and cambered wing of reference 1 might be questionable because of the difference in techniques. The ratio $\left[\frac{(L/D)_{max_{mod}}}{(L/D)_{max_{basic}}}\right]$, referred to as the performance ratio, therefore, has been presented in figures 10 and 11 and is believed to provide a more realistic basis for evaluating the effects of the wing modification. For the wing alone, the modification increased the performance ratio up to a Mach number of 0.95, but had little effect at higher speeds. When applied to the wing-fuselage configuration, the wing modification caused no gain in the performance ratio, throughout the Mach number range, which could possibly be due to the large increase in minimum drag caused by addition of the fuselage. The performance ratio of the twisted and cambered wing and wing-fuselage combinations of reference 1, obtained by adjusting the drag polars of that investigation to the $C_{D_{min}}$ values of this paper, are presented for comparison in figures 10 and 11. As can be seen by this comparison, the present modification to the wing did not prove as effective in improving the performance characteristics as did the twist and camber used in the wing in the investigation of reference 1. In this previous investigation, the twist and camber had been selected so as to provide a uniform loading at a lift coefficient of 0.25 and a Mach number 1.10.

The lift coefficient at which $(L/D)_{max}$ occurred usually was slightly higher for the modified wing configurations than for the flat wing configurations. Large Mach number effects on C_L for $(L/D)_{max}$ were indicated for all configurations investigated at Mach numbers between 0.95 and 1.10.

Pitching-Moment Characteristics

In general, the pitching-moment slopes $\partial C_m/\partial C_L$ were only slightly affected by the wing modification throughout the test range of Mach numbers. At the highest lift coefficients and high Mach numbers, the modification seemed to cause the wing alone to be slightly more unstable (fig. 6), whereas the wing-fuselage combination became slightly more stable (fig. 7).

The variations of the pitching-moment coefficient at zero lift C_{m_0} with Mach number were practically unaffected by the modification.

CONCLUSIONS

An investigation of the effects of partial-span leading-edge camber on the aerodynamic characteristics of a sweptback wing indicated the following conclusions:

1. For the wing-alone configuration, use of the partial-span leading-edge camber provided an increase in maximum lift-drag ratios up to a Mach number of 0.95, after which no gain was realized. For the wing-fuselage combination, the partial-span leading-edge camber appeared to cause no gain in maximum lift-drag ratio throughout the test range of Mach numbers.

2. The lift-curve slopes of the modified configurations indicated no significant change over the basic configurations in the subsonic range but resulted in slight reductions at the higher Mach numbers. No significantly large changes, due to the modification, in pitching-moment slopes or lateral center of additional loading were indicated. The modification resulted in a slight increase in minimum drag at the higher Mach numbers for the wing-alone configuration and the increase occurred throughout the Mach number range for the wing-fuselage configuration.

3. The partial-span leading-edge camber modification did not prove as effective in improving the performance characteristics as did twisting and fully cambering a wing of the same plan form in a previous investigation.

Langley Aeronautical Laboratory
National Advisory Committee for Aeronautics
Langley Field, Va.

REFERENCES

1. Spreemann, Kenneth P., and Alford, William J., Jr.: Investigation of the Effects of Twist and Camber on the Aerodynamic Characteristics of a 50° 38' Sweptback Wing of Aspect Ratio 2.98. Transonic-Bump Method. NACA RM L51C16, 1951.

2. Jones, J. Lloyd, and Demele, Fred A.: Aerodynamic Study of a Wing-Fuselage Combination Employing a Wing Swept Back 63°.- Characteristics Throughout the Subsonic Speed Range With the Wing Cambered and Twisted for a Uniform Load at a Lift-Coefficient of 0.25. NACA RM A9D25, 1949.

3. Donlan, Charles J., Myers, Boyd C., II, and Mattson, Axel T.: A Comparison of the Aerodynamic Characteristics at Transonic Speeds of Four Wing-Fuselage Configurations as Determined From Different Test Techniques. NACA RM L50H02, 1950.

TABLE I.-FUSELAGE and CANOPY ORDINATES

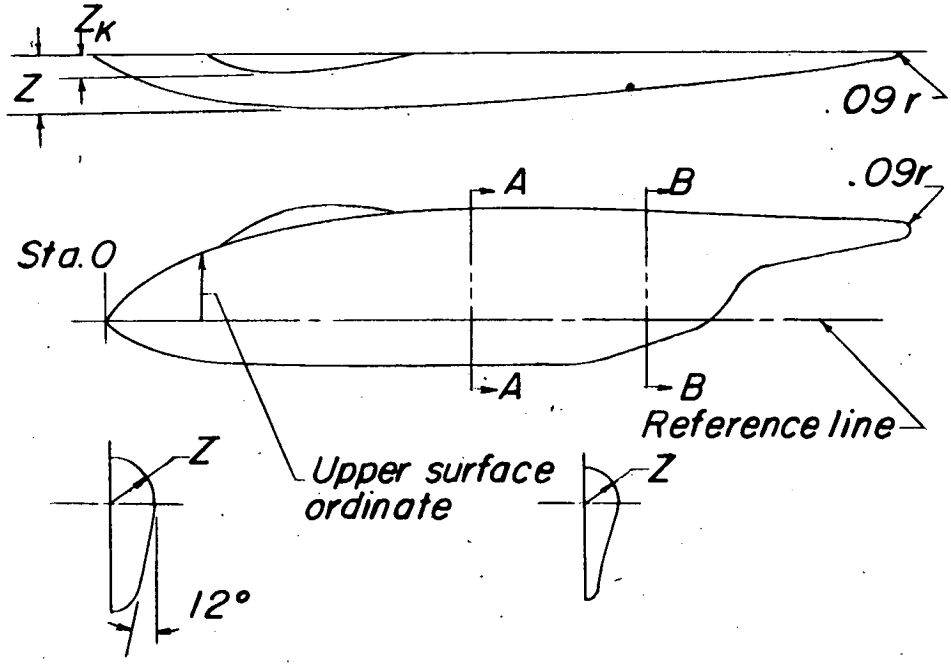

Section A-A Section B-B

r radius, inches

Fuselage Ordinates

Station (in.)	Upper Surface (in.)	Lower Surface (in.)	Z Radius (in.)
0	0	0	0
.47	.47	-.31	.29
.90	.72	-.44	.42
1.97	1.08	-.53	.54
3.05	1.26	-.53	.62
4.12	1.34	-.53	.61
5.20	1.35	-.53	.56
5.95	1.35	-.53	.56
6.27	1.34	-.43	.48
7.35	1.30	-.08	.37
7.56	1.30	.05	.37
7.78	1.30	.40	.37
7.99	1.30	.60	.37
8.42	1.26	.72	.27
9.50	1.21	.89	.15
9.71	1.19	.93	.13
9.98	1.10	1.10	0

Canopy Ordinates

Station (in.)	Upper Surface (in.)	Z_k (in.)
1.34	.89	0
2.13	1.34	.19
2.51	1.42	.17
3.05	1.42	.11
3.83	1.33	0

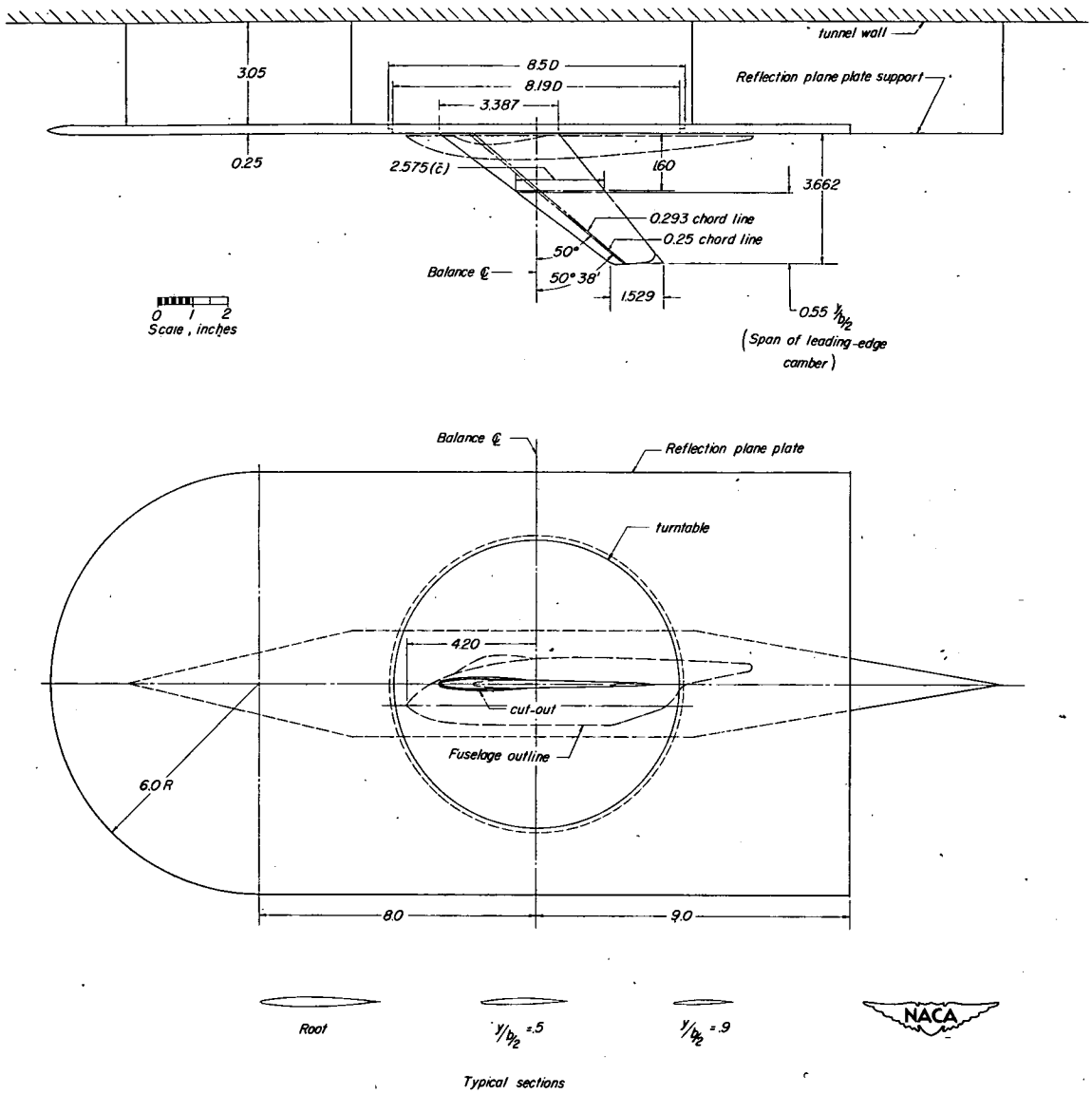

Figure 1.- Wing-alone configuration with 50° 38' sweptback wings, aspect ratio 2.98, taper ratio 0.45, and modified NACA 64A-series airfoil sections mounted on reflection plane.

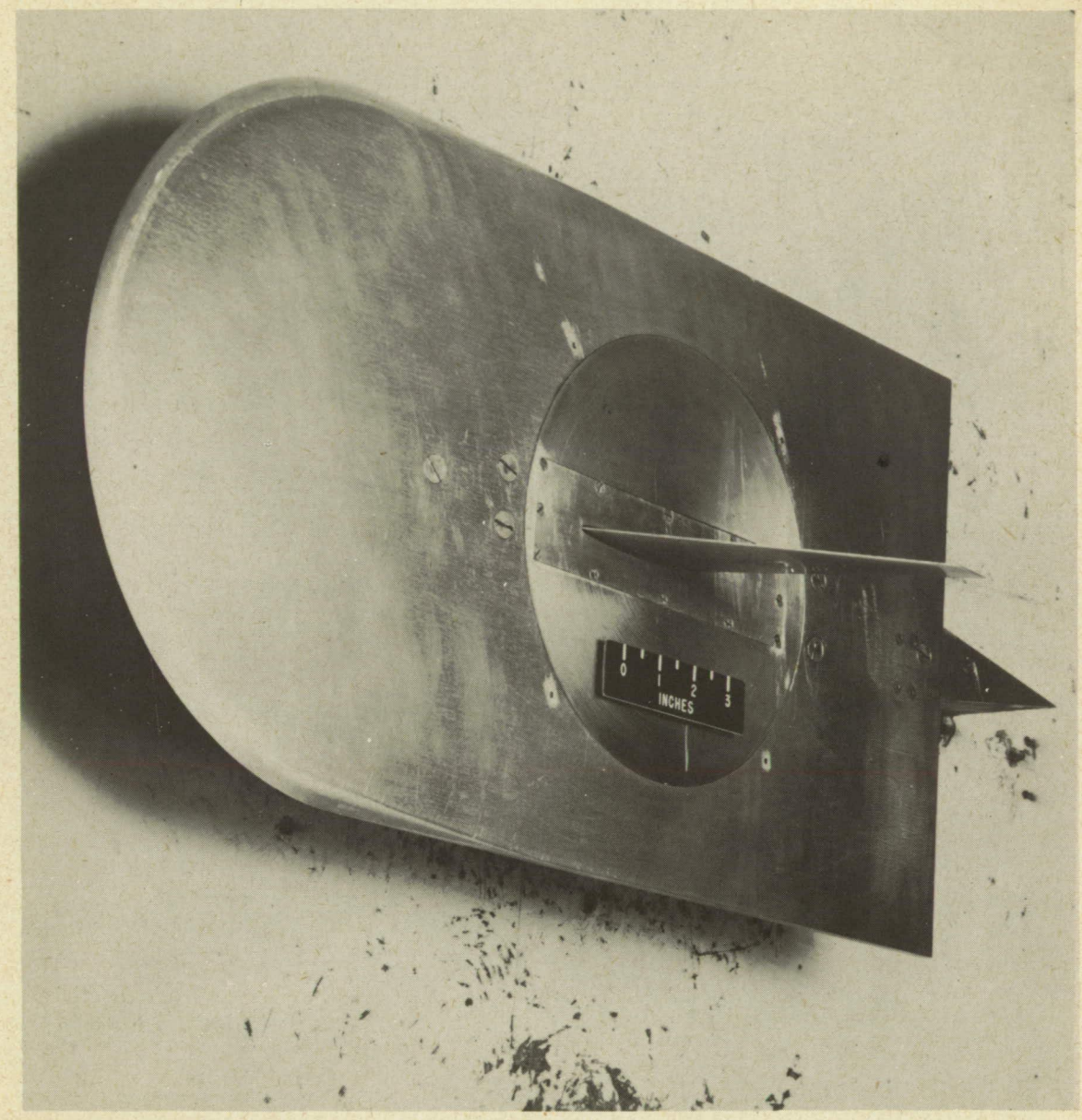

Figure 2.- Photograph of typical model and reflection-plane setup. NACA L-67368

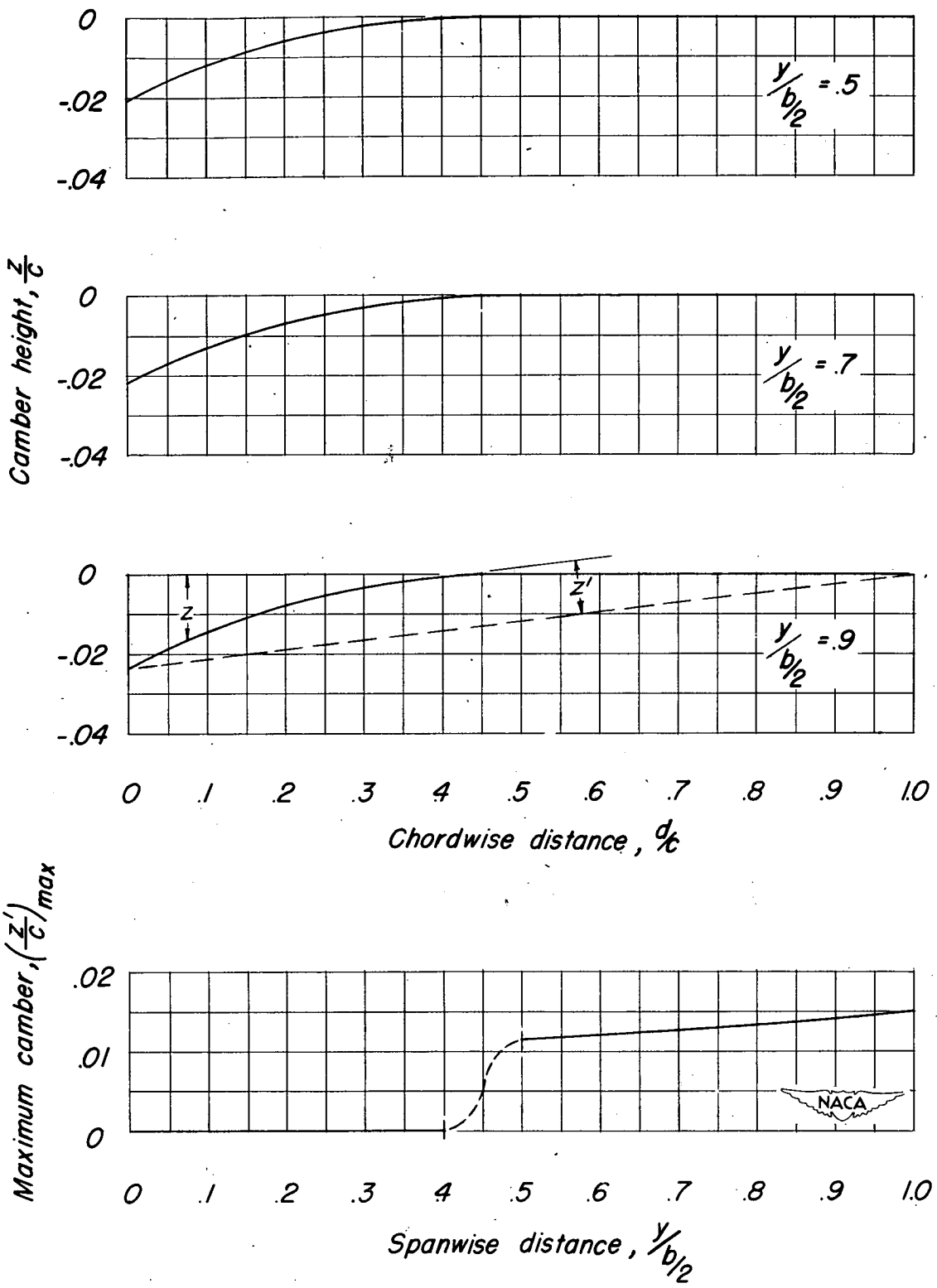

Figure 3.- Camber variations of wing with partial-span leading-edge camber.

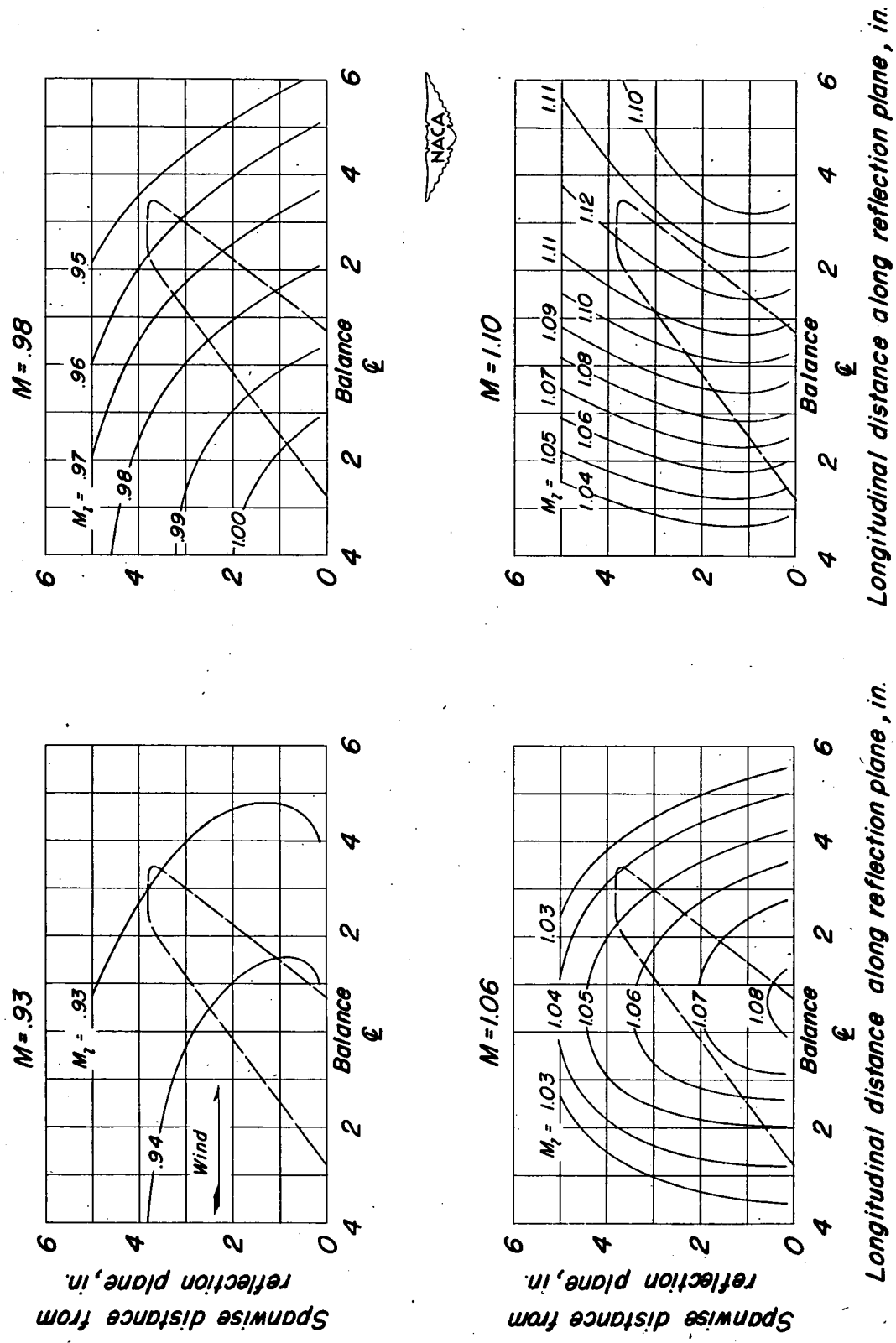

Figure 4.- Typical Mach number contours over reflection plane in model test region with no model in position.

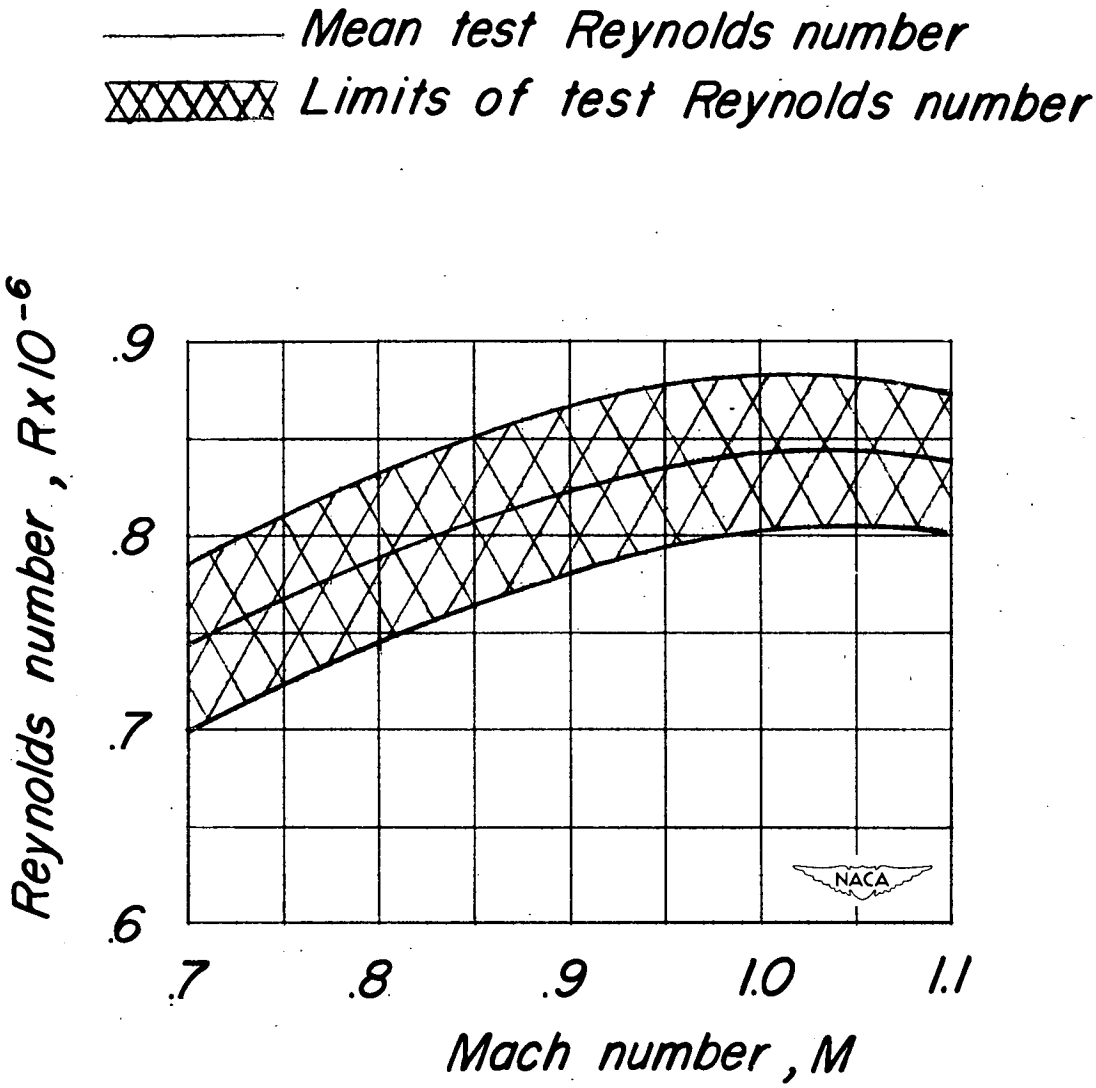

Figure 5.- Variation of test Reynolds number with Mach number.

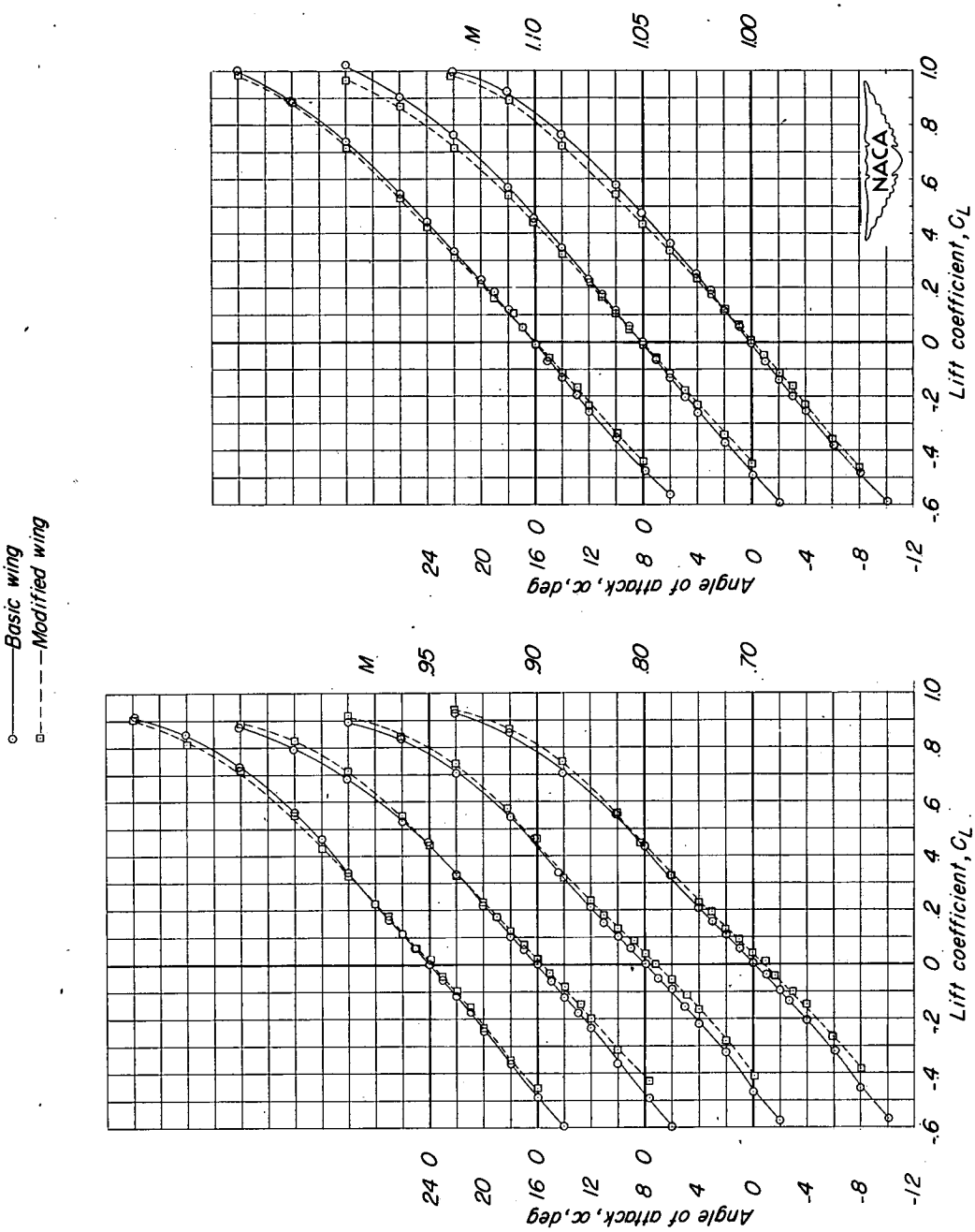

(a) α against C_L.

Figure 6.- Aerodynamic characteristics of the wing-alone test models.

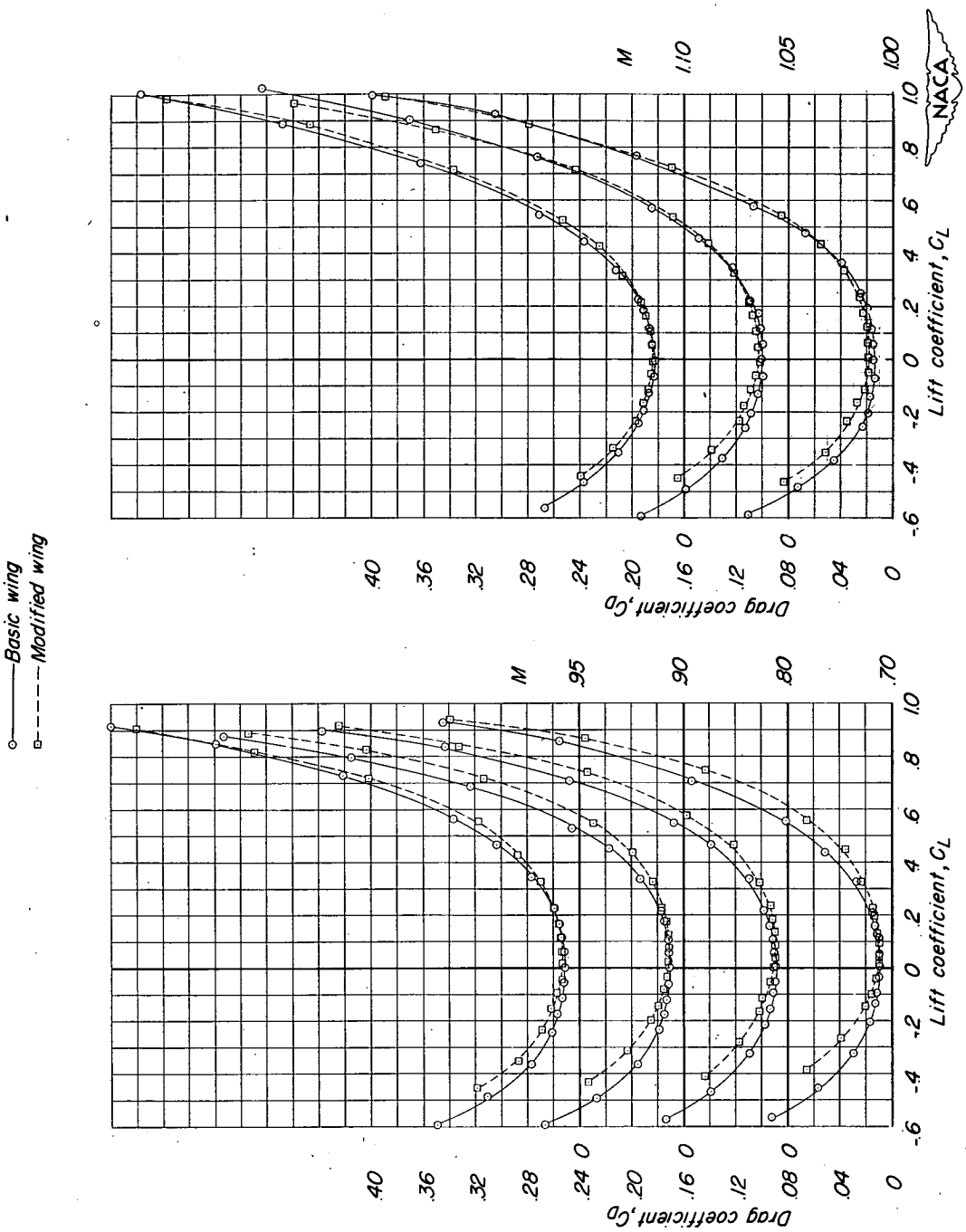

(b) C_D against C_L.

Figure 6.- Continued.

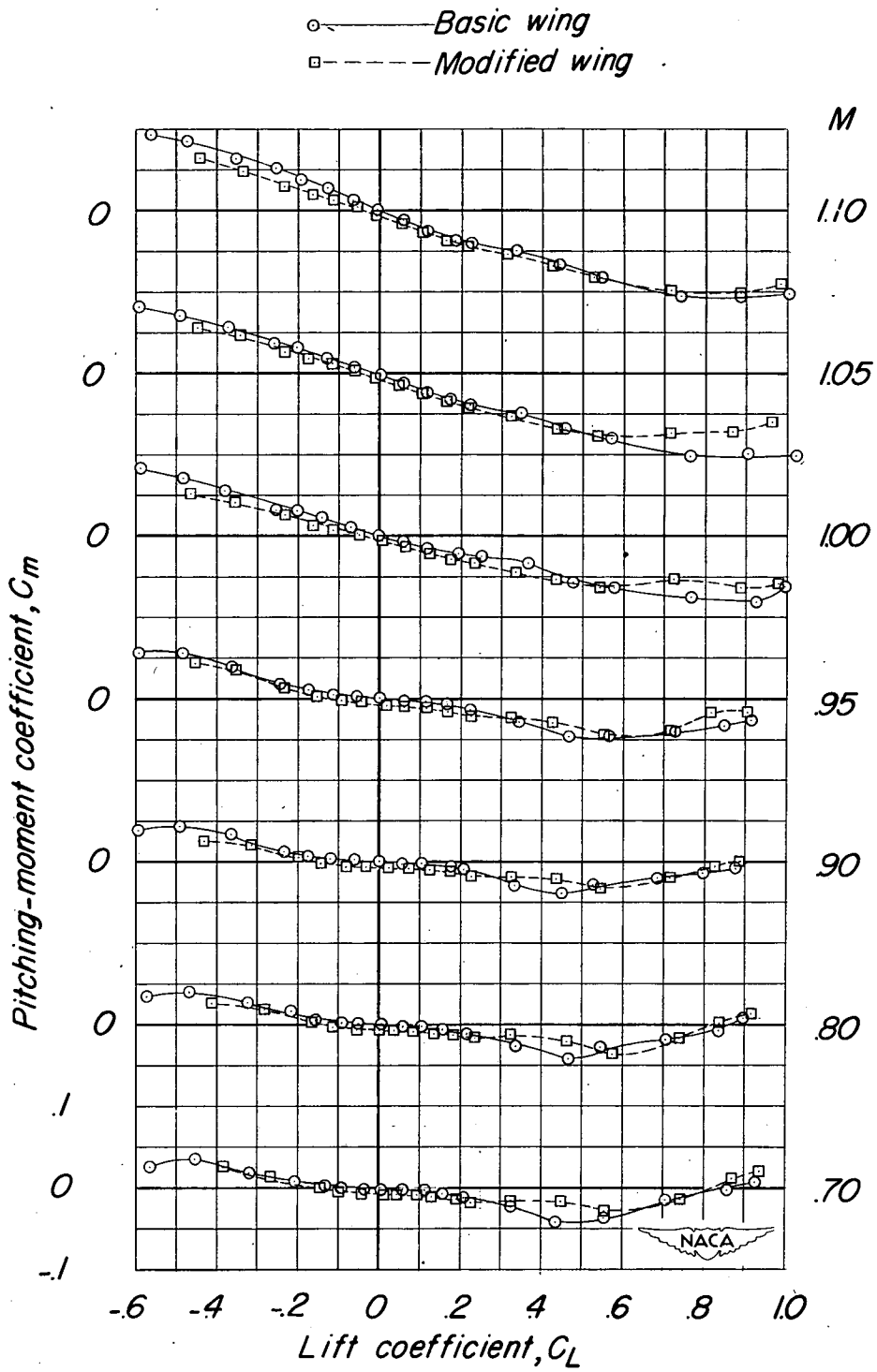

(c) C_m against C_L.

Figure 6.- Continued.

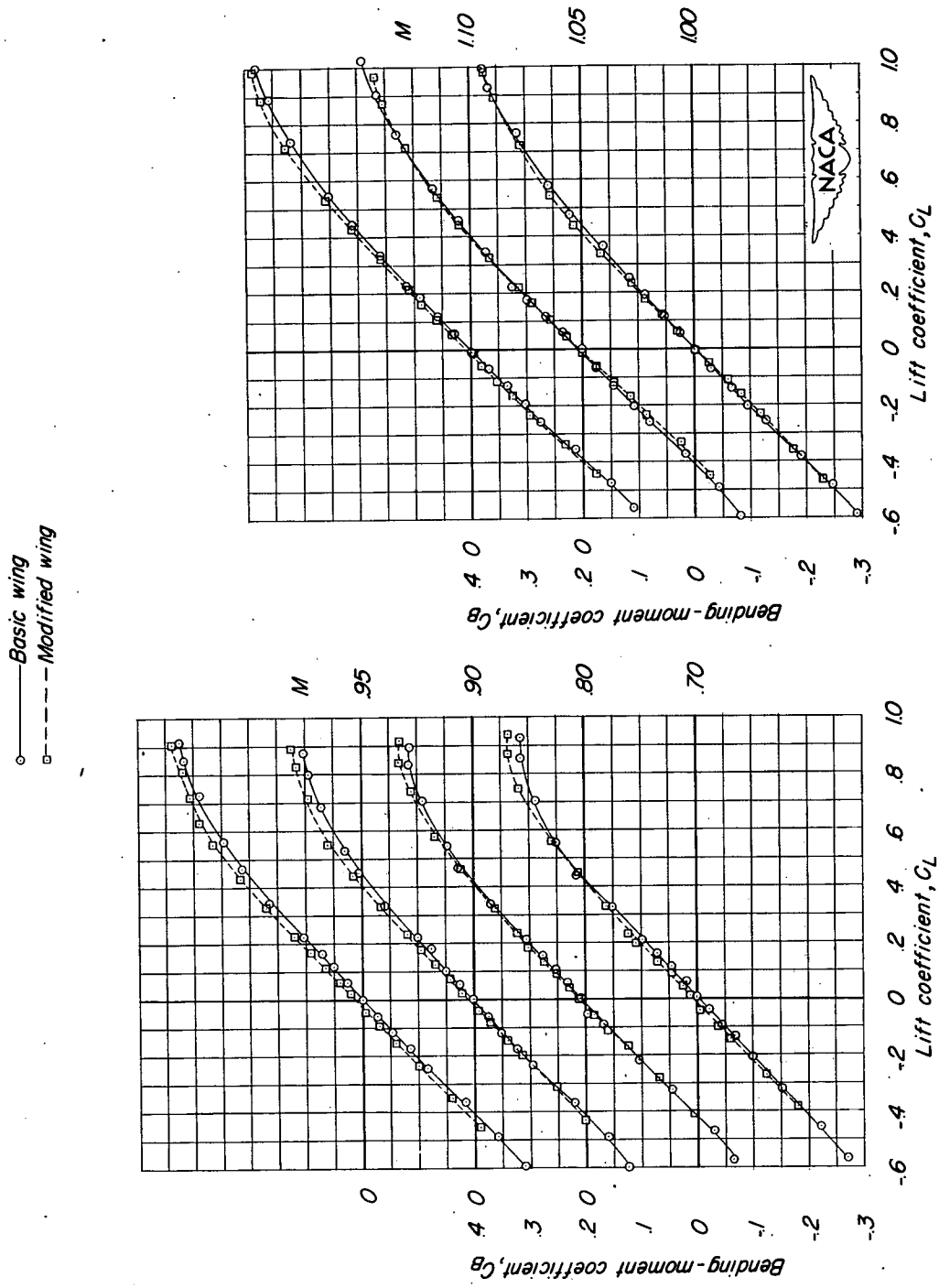

(d) C_B against C_L.

Figure 6.- Concluded.

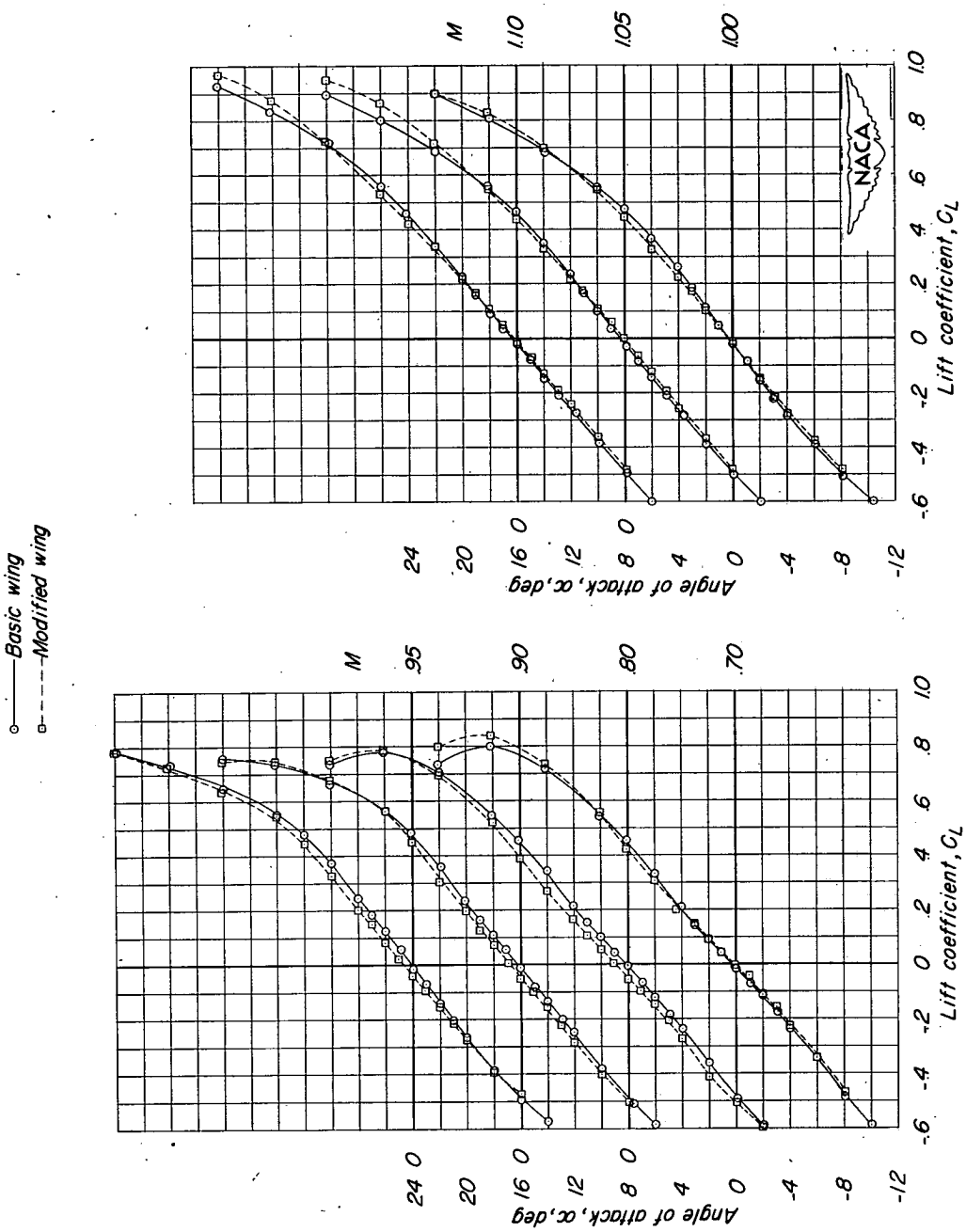

(a) α against C_L.

Figure 7.- Aerodynamic characteristics of the wing-fuselage test models.

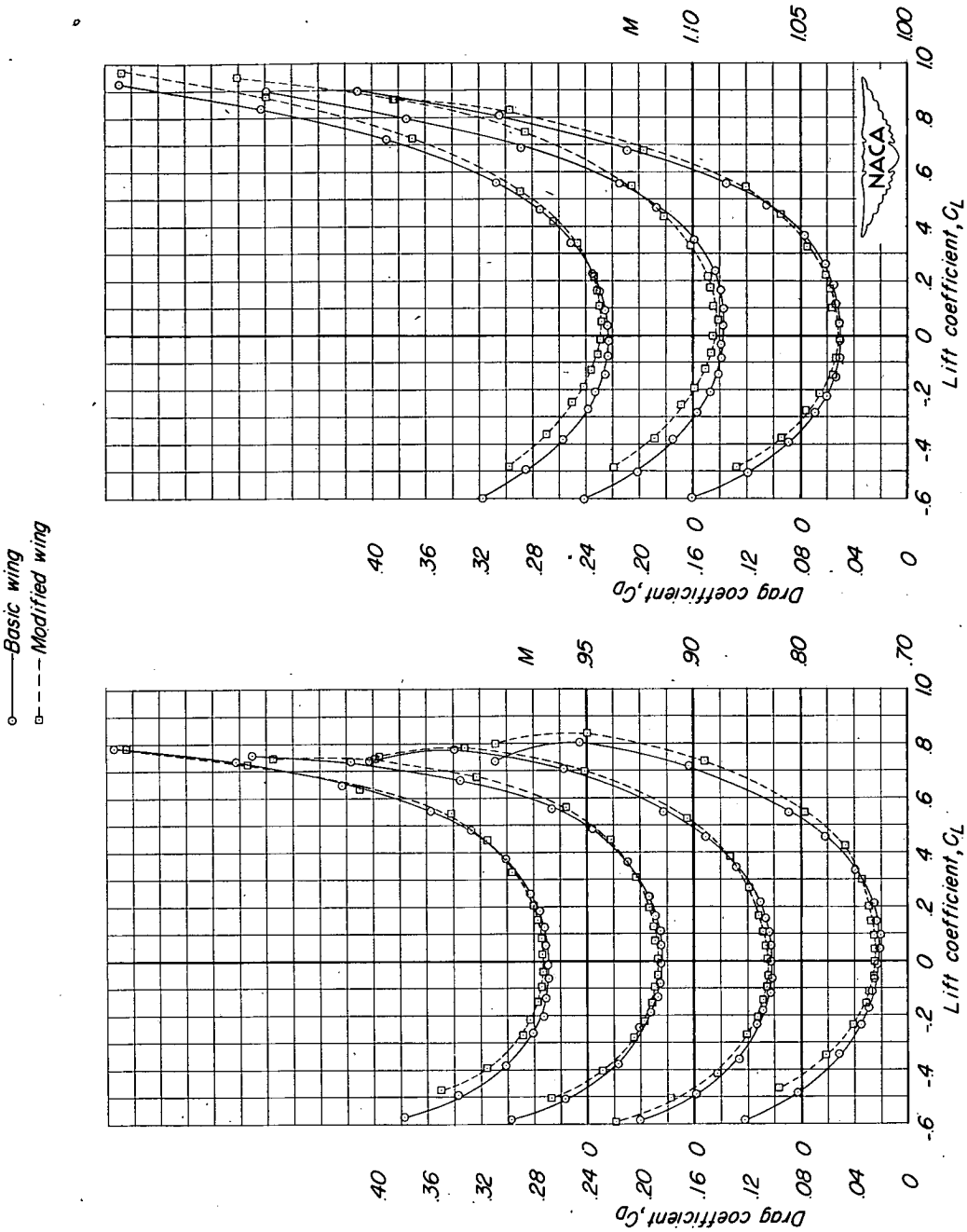

(b) C_D against C_L.

Figure 7.- Continued.

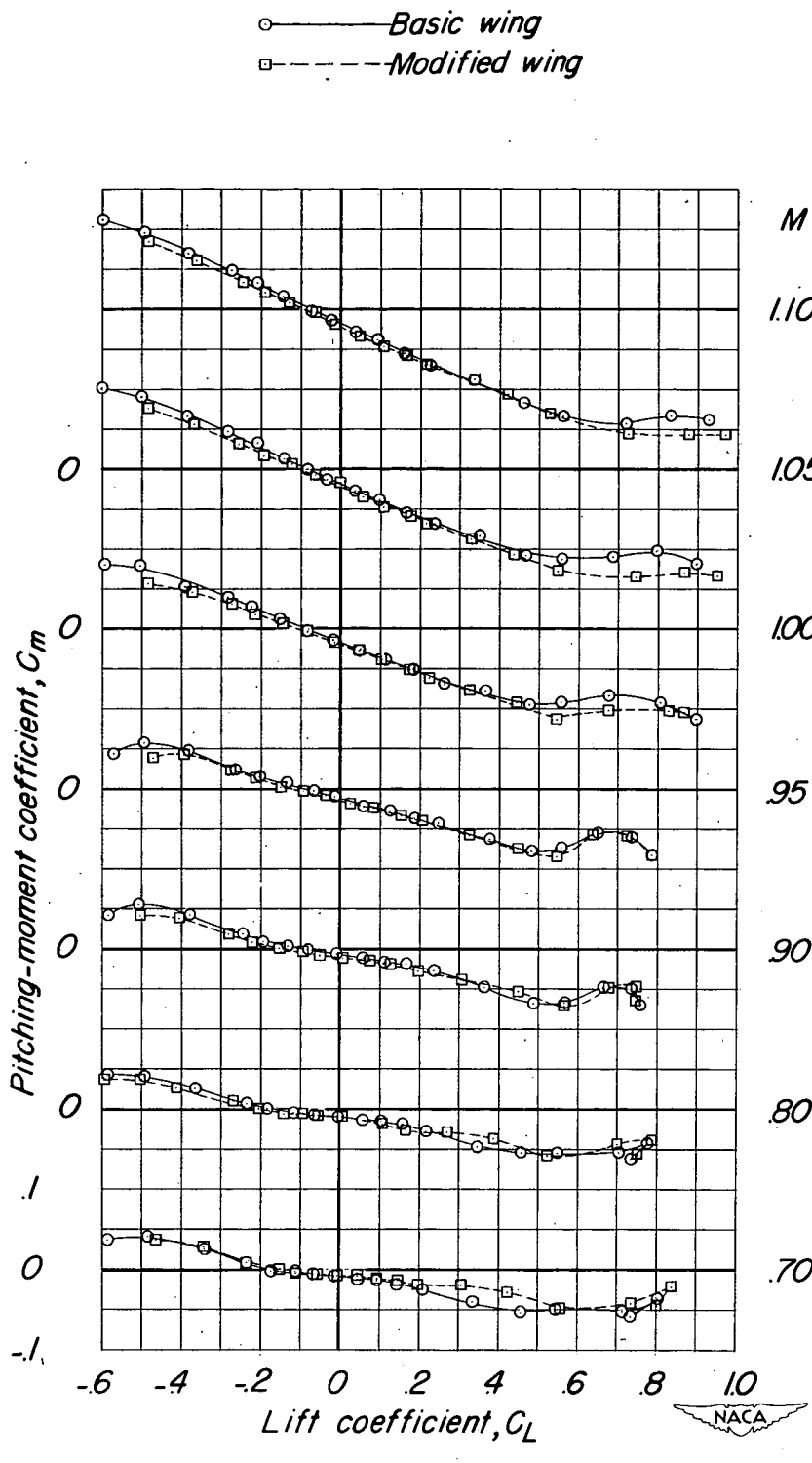

(c) C_m against C_L.

Figure 7.- Continued.

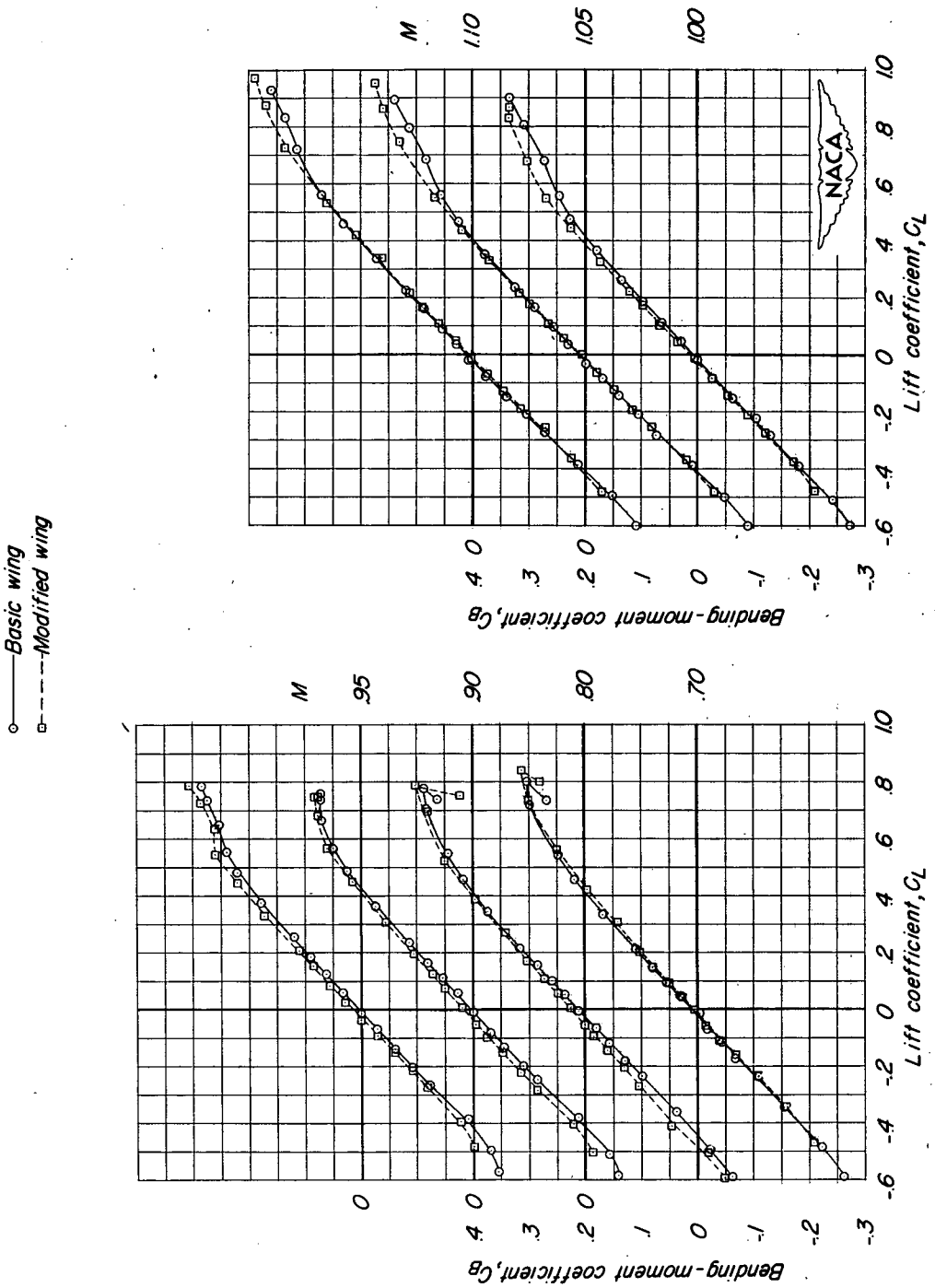

(d) C_B against C_L.

Figure 7.- Concluded.

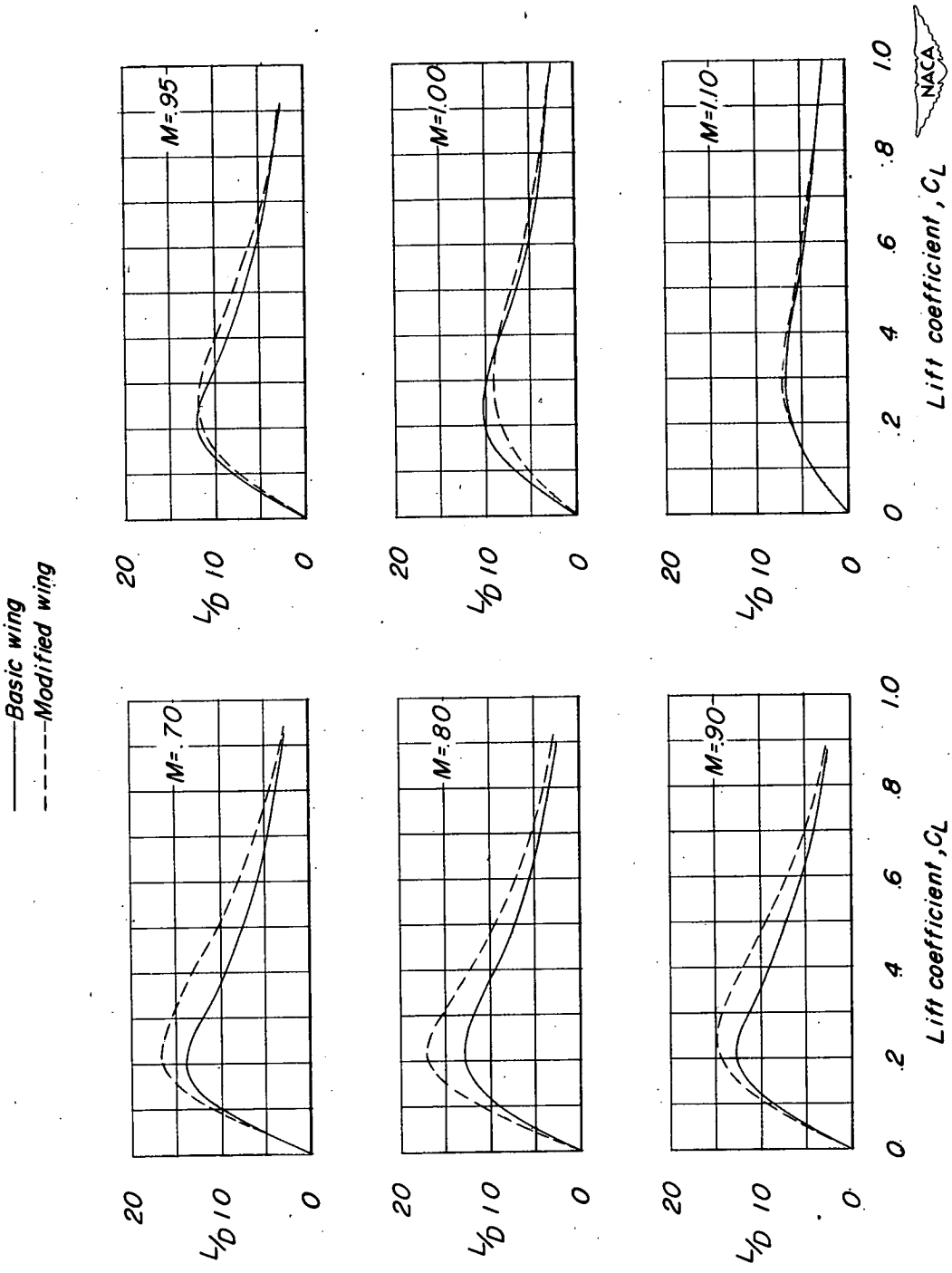

Figure 8.- Lift-drag ratios of the wing-alone test models.

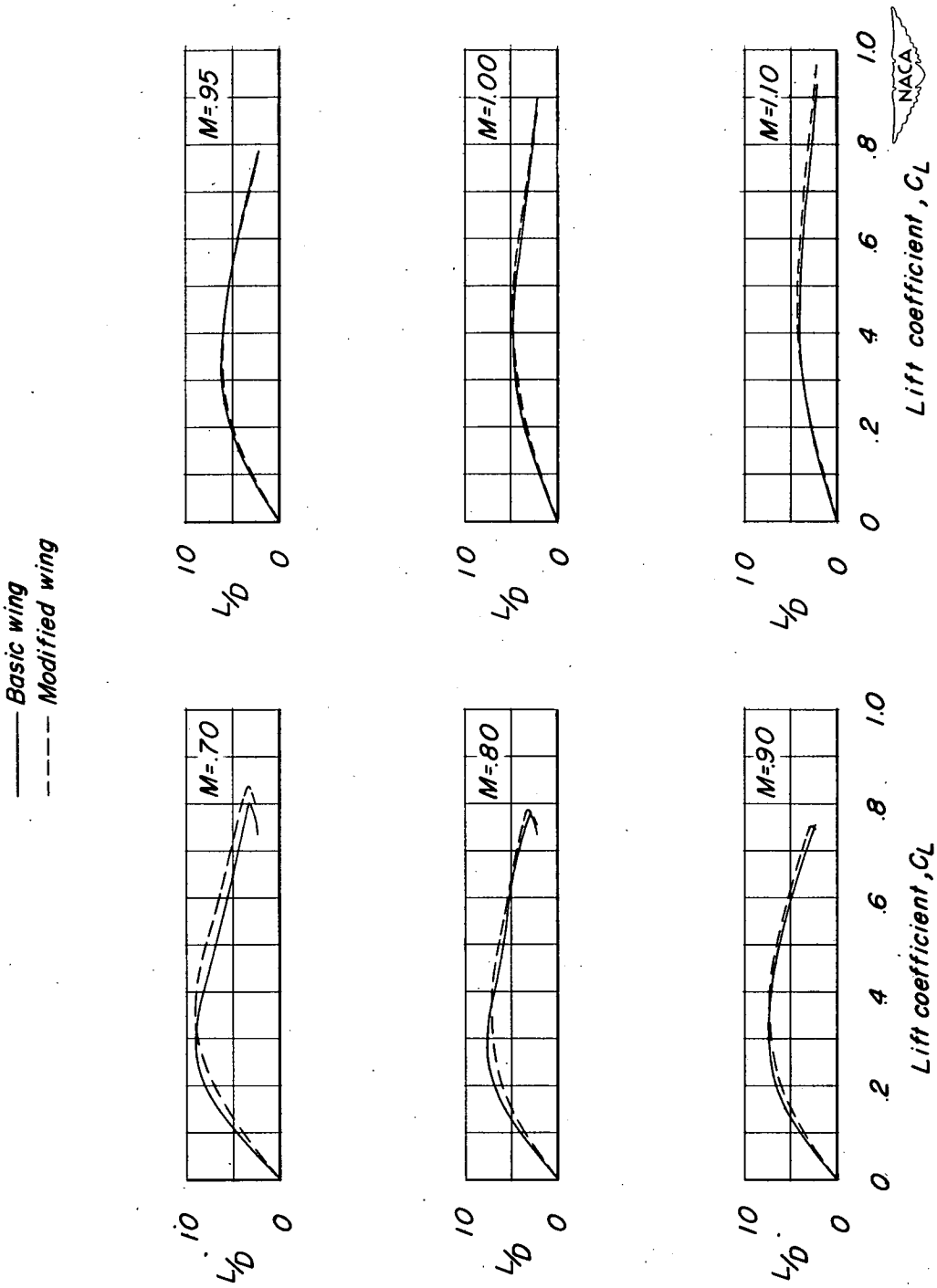

Figure 9.- Lift-drag ratios of the wing-fuselage test models.

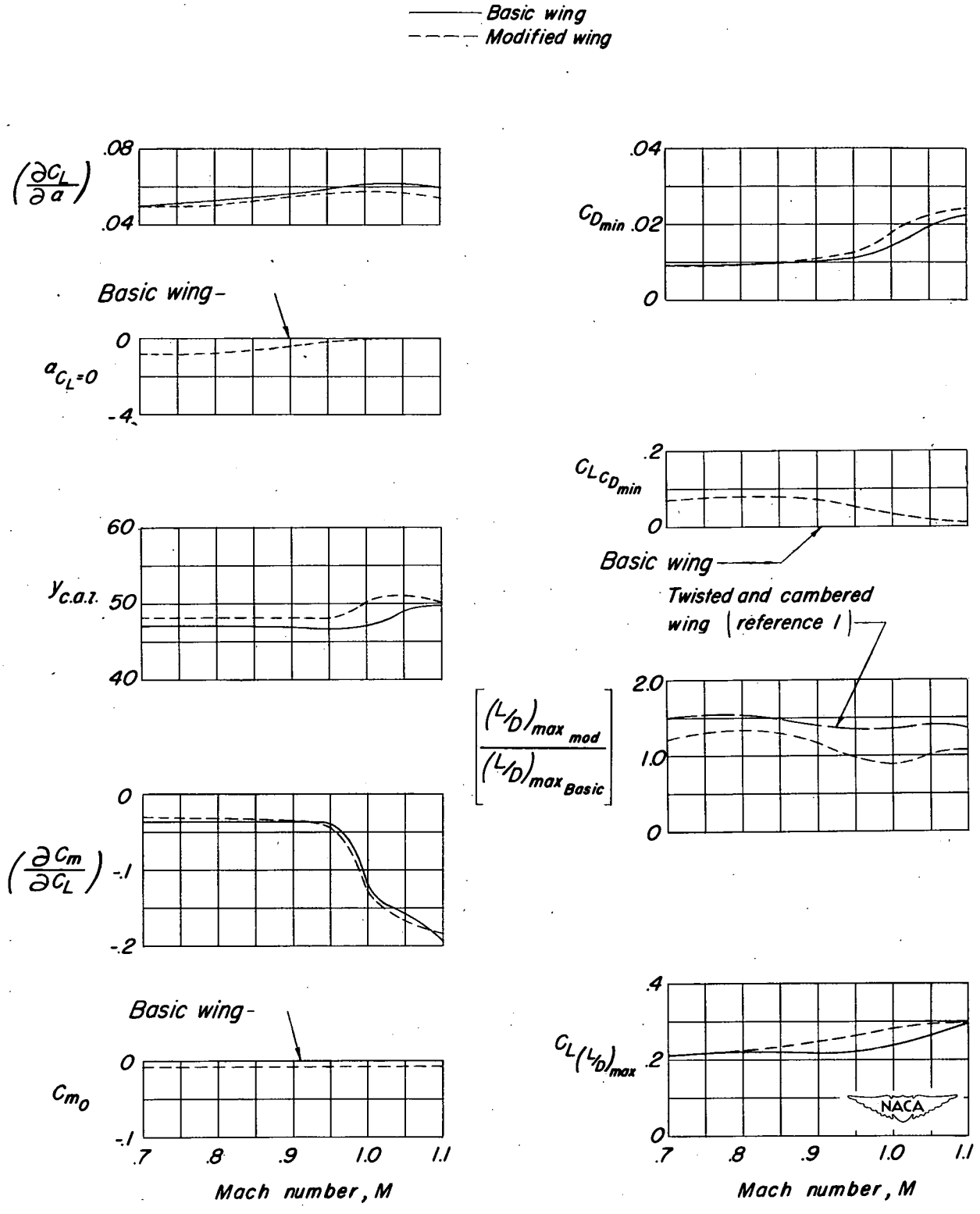

Figure 10.- Summary of the aerodynamic characteristics of the wing-alone test models.

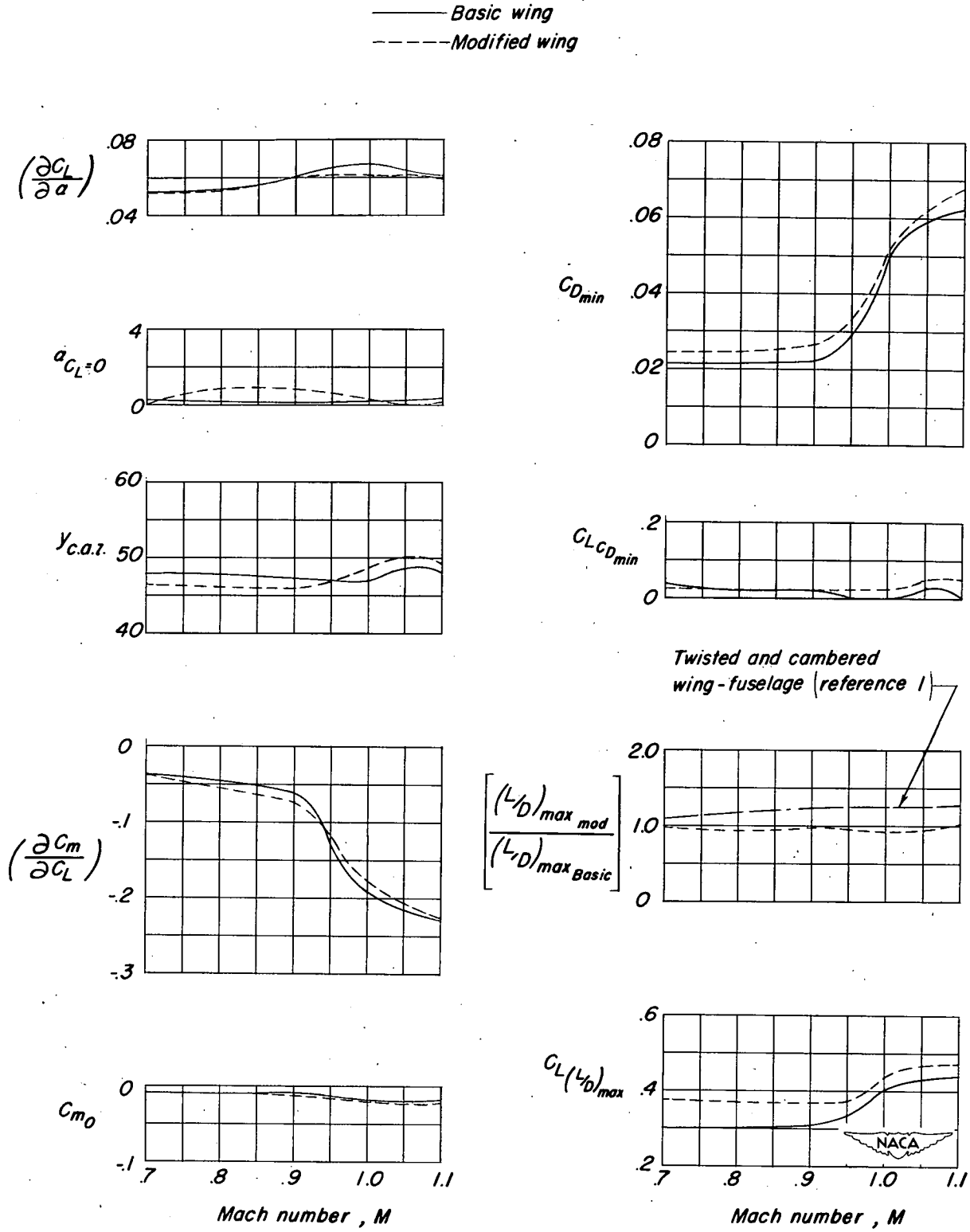

Figure 11.- Summary of the aerodynamic characteristics of the wing-fuselage test models.

NACA-Langley - 6-23-52 - 325

CONFIDENTIAL

CONFIDENTIAL